Nuclear Physics: A Key Ingredient in Astrophysical Modeling

F.-K. Thielemann, D. Argast, F. Brachwitz, J.L. Fisker, C. Fröhlich, R. Hirschi, E. Kolbe, D. Mocelj, T. Rauscher [a] *

[a]Department of Physics & Astronomy, Univ. of Basel, Klingelbergstrasse 82, CH-4056 Basel, Switzerland

Nuclear physics is a basic ingredient in a large number of energetic astrophysical environments which are characterized by sufficient temperatures and densities to permit scattering events among particles, leading to nuclear reactions and possibly the production of unstable reaction poducts. Strong, electromagnetic and weak interactions (fusion, exchange reactions, photodisintegrations, beta-decays, electron [and positron] captures on nucleons and nuclei, neutrino scattering and captures [i.e. neutral and charged current reactions]) can produce nuclei far form stability and require extended knowledge of nuclear structure near and far from stability, including decay and fission properties. Last, but not least, the nucleon-nucleon interaction determines the nuclear equation of state at and beyond nuclear densities and is ultimately connected to the question under which conditions a phase transitions from hadrons to the quark-gluon plasma occurs. In this review we will survey how these aspects of nuclear physics enter the modeling of astrophysical objects.

1. Introduction

Computational modeling of astrophysical objects requires the combined treatment of different subfields of physics for a complete description: 1. hydrodynamics/hydrostatics for the modeling of mass flows, 2. energy generation and nucleosynthesis for understanding the composition changes due to nuclear reactions and the related energy releases, 3. energy transport via conduction, radiation or possibly convection, and finally 4. thermodynamic properties of the matter involved, especially the equation of state which creates a direct relation between energy release and hydrodynamic response via pressure and entropy. In this introduction we address these four topics by highlighting the role and impact of nuclear physics in each of these aspects of stellar modeling (for big bang nucleosynthesis see [51,47]) and give a short review of stellar evolution before concentrating on explosive events.

1.1. Modelling Astrophysical Objects

Hydrodynamics is mostly a question of the computational technics employed, the required resolution to model the physics correctly, and the approximations permitted for

*supported by Swiss NSF grants 20-06831.02 and 20-105328/1

an appropriate description of the system. These can include 1D (mostly spherically symmetric) [162] vs. 2D and 3D simulations [114,202,99,146,69], multigrid or adaptive grid methods for providing the necesseary resolution [58,142,65], implicit vs. explicit numerical methods dependent on the dynamical timescales of the system and duration of the evolution intended to be covered [95,105,142], the possible effect of rotation, the question whether Newtonian hydrodynamics is sufficient to describe the problem or whether the strength of the gravitational field requires general relativity [140,177,55,178]. All of this could be complicated by the existence of electric and magnetic fields which require the application of magneto-hydrodynamic equations instead of pure hydrodynamics [138,106]. For the issues discussed above there exists no direct relation to nuclear physics properties, unless one considers how timescales of nuclear energy release can enter hydrodynamic modeling.

Energy generation and nucleosynthesis depend strongly on the nuclear reactions occurring in a stellar environment. However, different stellar environments imply also different kinds of nuclear physics knowledge. In stellar evolution all types of fusion reactions are required which transform hydrogen to iron-group nuclei via hydrogen, helium, carbon, neon, oxygen and silicion burning, releasing eventually 8.7 MeV of binding energy per nucleon. The composition changes in stellar evolution, occurring on timescales of millions to billions of years rather than timescales of the strong interaction are dominated by reactions which can barely proceed for the temperatures involved. The latter correspond to typical bombarding energies below the Coulomb barrier. Such reactions require high intensity, (very) low energy beams and either passive or active shielding [23,118,250].

Reactions occuring in explosive environments experience higher temperatures and thus higher energies and larger cross sections. The fact that shorter explosive timescales permit reactions with unstable nuclei before their decay makes it necessary to investigate also cross sections with unstable nuclei. For experimental methods and reviews see e.g. ref.[118,4,108,134], for theoretical predictions involving nuclei at excitations with a sufficiently high density of states see [198–200,54,**?**], and for weak interactions see [133,127]. Many explosive environments with fuels of N≈Z produce also unstable nuclei close to stability. However, esplosive environments with a large surplus of hydrogen (protons) permit proton captures up to the proton dripline. This gives rise to the so-called rp-process (rapid proton capture). Very neutron-rich environments permit neutron-captures up to the neutron dripline and are the sites of the r-process (rapid neutron capture).

Low and intermediate temperatures require individual cross sections to follow the reaction flows. High temperatures lead to chemical equilibria. In the case of the rp- and r-process this causes abundance distributions on isotonic or isotopic lines which show maxima at specific proton or neutron separation energies. Therefore, in such cases individual reactions might not be that important, but such equilibria depend on correct reaction Q-values or separation energies, i.e. the proper knowledge of nuclear masses far from stability. The behavior of shell effects and shell closures deserves special attention [187]. Another aspect in the r-process is related to fission barriers and fission yields for nuclei far from stability [19,184]. The tendency in recent years is here to move from macroscopic-microscopic models like the droplet model to non-relativistic or relativistic mean field methods and even shell model calculations, if the model space permits this [163,56,150,18,203,244,210].

While strong interaction timescales can support equilibria at high temperatures (and densities), weak interactions lead very seldom to chemical equilibria. Exceptions are early phases of the big bang and equilibrated (cooled) neutron stars. Thus, it is always necessary to follow each individual weak interaction, i.e. beta-decays, electron captures and neutrino-nucleon/nucleus interactions. The present state of the art calculations for beta-decays are QRPA or shell model calculations [164,150,25], electron capture caclulations are now possible within the shell model up to the pf-shell, i.e. the important Fe-group nuclei [133]. The best calculations for neutrino-nucleus cross sections are available within the continuum RPA (CRPA) model [127].

Energy transport in stellar environments occurs by a variety of modes which can be categorized in two major schemes: mixing/convection of matter with a given heat content or transport via radiation. The first category involves all types of hydrodynamic instabilities from convection due to entropy inversion in regular stellar evolution [86] to Rayleigh-Taylor instabilities in dynamic events [169,170,17,123] and rotationally induced meridional circulation [147]. Radiation transport is in most phases of stellar evolution related to photons and in that respect governed by photon scattering and reaction processes. Photon-ion interactions with bound-bound and bound-free transitions are covered in atomic physics and generally addressed as opacities. In a similar way photon-electron interactions enter [205,213].

Nuclear physics is addressed when "radiation" transport proceeds by the way of neutrinos in hot neutron star evironments, be it in stellar collapse in supernovae or events which involve hot neutron stars collapsing to black holes (either in massive stars or in neutron star mergers) [161,143,146]. Here the cross sections of neutrino-nucleus, neutrino-nucleon, neutrino-nuclear matter and neutrino-electron/positron collisions are relevant and the quest is to perform precise calculations [32,36,188,37].

Convection and radiation transport are both closely linked to the numerical treatment of hydrodynamics. How are convective flows modeled in 1D vs. multi-D hydro? Which methods are employed to perform radiation transport, independent on the micro-physics related cross sections involved [143,146]?

Thermodynamics is an aspect also coupled strongly to hydrodynamics, as the pressure due to the equation of state enters directly into the formation of shock waves, the entropy enters into the formation of hydrodynamical instabilities and convection. In the outer zones of a star, especially the atmosphere, the EOS is mainly given by atomic physics via the mixture of a partially ionized ion, electron, and photon gas [52]. In deeper layers ions are fully ionized and the thermalized Fermi gases (e.g. electron/positron), Bose gases of massless particles (i.e. Planck distributions of photons) and Boltzmann distributions of nuclei are needed. Here nuclear physics enters only indirectly by possibly governing the reactions which provide the composition of nuclei and the total amount of electrons available, the latter being dependent on electron captures and weak interactions in general.

A more direct involvement of nuclear physics is given for the EOS at and beyond nuclear densities [137,247,215,135]. Important features are the different stages of dissolving nuclei into a nucleon soup (involving a number of topologies) and the creation of new particles at supranuclear densities. When do hyperons occur (sigmas, lambdas at $2 \times \rho_0$?), do we have a formation of kaon or pion condensates, at what density does the quark-hadron

phase transition occur (4-5$\times\rho_0$?) [247,189,178]?

After this short general introduction and overview, we want to give a number of specific astrophysical applications to show how the different nuclear aspects enter in the modeling of these stellar events. This addresses mostly explosive events, like type Ia and type II supernovae (SNe Ia and SNe II), the features and possible sites of the r-process, as well as novae and X-ray bursts, the sites of explosive H-burning and the rp-process. In order to provide the background for the stellar objects involved, we give here a brief summary of stellar evolution.

1.2. Stellar Evolution, Setting the Stage for Explosions

H-burning converts of ^{1}H into ^{4}He via pp-chains or the CNO-cycles. The simplest PPI chain is initiated by $^1\mathrm{H}(p,e^+\nu)^2\mathrm{H}(\mathrm{p},\gamma)^3\mathrm{He}$ and completed by $^3\mathrm{He}(^3\mathrm{He},2\mathrm{p})^4\mathrm{He}$. The dominant CNOI-cycle chain $^{12}\mathrm{C}(\mathrm{p},\gamma)^{13}\mathrm{N}(e^+\nu)^{13}\mathrm{C}(\mathrm{p},\gamma)^{14}\mathrm{N}(\mathrm{p},\gamma)^{15}\mathrm{O}(e^+\nu)^{15}\mathrm{N}(\mathrm{p},\alpha)^{12}\mathrm{C}$ is controlled by the slowest reaction $^{14}\mathrm{N}(p,\gamma)^{15}\mathrm{O}$. (The solar neutrino puzzle with an appearent contradiction between the prediction of ν_e-fluxes from solar models and neutrino observatories has only recently been resolved via neutrino oscillations observed with SNO [3] and KAMLAND [59]. The $^7\mathrm{Be}(p,\gamma)$-cross section still serves as a constraint for the mixing angle.)

Further burning stages are characterized by their major reactions, which are in He-burning $^4\mathrm{He}(2\alpha,\gamma)^{12}\mathrm{C}$ (triple-alpha) and $^{12}\mathrm{C}(\alpha,\gamma)^{16}\mathrm{O}$, in C-burning $^{12}\mathrm{C}(^{12}\mathrm{C},\ \alpha)^{20}\mathrm{Ne}$, and in O-burning $^{16}\mathrm{O}(^{16}\mathrm{O},\alpha)^{28}\mathrm{Si}$. The alternative to fusion reactions are photodisintegrations which start to play a role at sufficiently high temperatures when $30kT{\approx}Q$ (the Q-value or energy release of the inverse capture reaction). This ensures the existence of photons with energies $>Q$ in the Planck distribution and leads to Ne-Burning [$^{20}\mathrm{Ne}(\gamma,\alpha)^{16}\mathrm{O}$, $^{20}\mathrm{Ne}(\alpha,\gamma)^{24}\mathrm{Mg}$] at $T{>}1.5\times10^9$K (preceding O-burning) due to a small Q-value of ≈4 MeV and Si-burning at temperatures in excess of $3{\times}10^9$K (initiated like Ne-burning by photodisintegrations [of ^{28}Si]). The latter ends in a chemical equilibrium with an abundance distribution around Fe (nuclear statistical equilibrium, NSE), as typical Q-values of 8-10 MeV permit photodisintegrations and also the penetration of the corresponding Coulomb barriers at these temperatures.

Stars with masses $M{>}8\mathrm{M}_\odot$ develop an onion-like composition structure, after passing through all hydrostatic burning stages, and produce a collapsing core at the end of their evolution, which proceeds to nuclear densities [172,253,44,86–88]. Less massive stars experience core H- and He-burning and end as C/O white dwarfs after strong episodes of mass loss [85]. These do not exceed the Chandrasekhar mass, i.e. the maximum stellar mass stabilzed against contraction due to the pressure of the degenerate electron gas.

The major uncertainties in all these hydrostatic burning stages are related to low energy fusion reactions, i.e. the cross sections at sub Coulomb barrier energies, where (until recently) a determination could be only obtained by extrapolation to low energies. The status of reactions has been discussed extensively [118,2,4,108] The main breakthrough in recent years is due to the possibility of measuring cross sections at stellar thermal energies in underground laboratories (LUNA) [23]. A number of uncertain reactions at low energies still wait to be explored. Among them are in H-burning $^7\mathrm{Be}(p,\gamma)^8\mathrm{B}$ (pp-chains), $^{14}\mathrm{N}(p,\gamma)^{15}\mathrm{O}$ (CNO-cycle), in He-burning $^{12}\mathrm{C}(\alpha,\gamma)^{16}\mathrm{O}$, $^{16}\mathrm{O}(\alpha,\gamma)^{20}\mathrm{Ne}$, n-production in He-burning (s-process) $^{22}\mathrm{Ne}(\alpha,n)^{25}\mathrm{Mg}$, $^{13}\mathrm{C}(\alpha,n)^{16}\mathrm{O}$, in C-

burning ^{12}C(^{12}C,p)^{23}Na, ^{12}C(^{12}C,α)^{20}Ne and in O-burning ^{16}O(^{16}O,p)^{31}P, ^{16}O(^{16}O,α)^{28}Si.

Extensive reviews exist over the major and minor reaction sequences in all burning stages in massive stars [10,227,253,8,94,102,201]. For a general overview of the s-process, which produces nuclei up to Pb and Bi via sequences of (slow) neutron captures and beta-decays during core and (dominantly) shell He-burning, see [115,116,72,117,38,241,242]. The late phases of stellar evolution (O- and Si-burning) are less prone to cross section uncertainties from strong interactions due to the emergence of equilibria, as discussed above. However, the high densities result in partially or fully degenerate electrons with increasing Fermi energies [172]. When these supercede the Q-value thresholds of electron capture reactions, this allows for electron capture on an increasing number of initially Si-group and later Fe-group (pf-shell) nuclei. While sd-shell reactions were well understood in the past [70], O-burning results are quite safe. The recent progress in pf-shell rates [133] led to drastic changes in the late phases of Si-burning [88], thus also setting new conditions for the subsequent Fe-core collapse after Si-burning, the size of the Fe-core and its electron fraction Y_e=$<Z/A>$.

2. Typa Ia Supernovae

2.1. The Mechanism

The basic recipe for SN Ia explosions is simple. A white dwarf in a binary system, growing via mass accretion from transfer from the companion star towards the limiting Chandrasekhar mass, contracts and ignites under degenerate (electron gas) conditions, causing a thermonuclear runaway [96,176,175,145,100]. Burning 1.4 $M_\odot$ of ^{12}C and ^{16}O in equal proportions to 1.398776 $M_\odot$ of ^{56}Ni releases the mass difference in nuclear binding energy, i.e. a thermonuclear explosion of about about 2.19×10^{51} erg, which disrupts the original white dwarf completely [173,255]. The subtraction of the gravitational binding energy of the white dwarf of ($\approx (5-6)\times10^{50}$ erg), plus the observed fact that not all material is burned to Fe/Ni (rather to intermediate elements like Mg, Si, S, Ca), leads to the observed explosion energies ($\approx 1.3\times10^{51}$ erg). The decay chain ^{56}Ni$\rightarrow^{56}$Co$\rightarrow^{56}$Fe can explain the lightcurve. A detailed analysis of observed lightcurves and spectra reveals the density and composition structure [248,100,28] and underlines that in normal, bright SNe Ia the CO white dwarf is almost fully burned. The complete thermonuclear disruption of the white dwarf produces predominantly Fe-group elements, on average of the order 0.6-0.8 $M_\odot$, and smaller amounts of Si, S, Ar, and Ca.

The mass accretion rate from the binary companion determines the central ignition density in spherically symmetric models, however the initial white dwarf mass, its C/O ratio, and its metallicity might enter as well [97,240,98,57]. Rotation and multi-D effects complicate this further [99,202,239,258].

The flame front propagates initially at a subsonic speed as a deflagration wave due to heat transport across the front. The flame thickness is given by heat conduction via the electron mean free path and is of the order 10^{-4}cm [237]. Hydrodynamic instabilities on various scales lead to a geometric enlargement of the flame surface or convective turnover of hot burned and cold unburned matter which enhances the averaged spherical flame speed over the one obtained with one dimensional heat conduction, i.e. laminar flame fronts [92,73,204]. Multi-dimensional hydro simulations suggest a deflagration speed $v_{\rm def}$

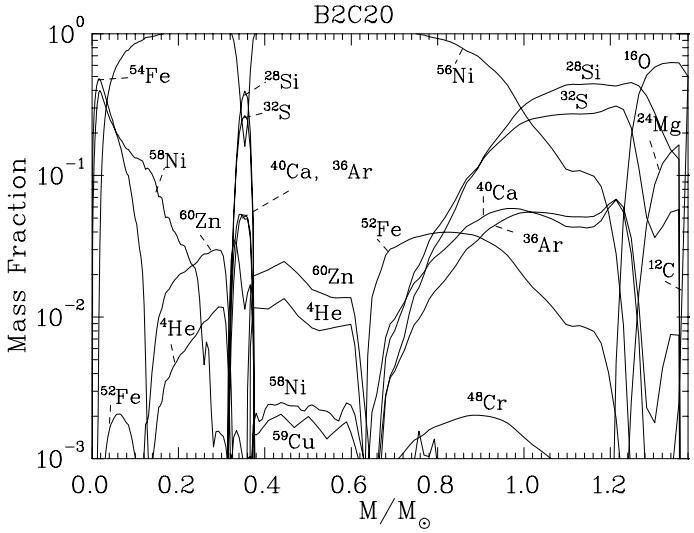

Figure 1. Isotopic composition for the layers of a type Ia supernova [27,232], starting thermonuclear burning with a deflagration front which turns into a detonation at 0.32 $M_\odot$. This is shown in the ^{56}Ni feature which sandwiches explosive O-burning products like ^{28}Si through ^{40}Ca. $M(r)$ indicates the radially enclosed mass, integrated from the stellar center. We see the products of explosive Si-burning (^{56}Ni), O-burning (^{28}Si), Ne-burning (^{16}O and ^{24}Mg), and minor amounts of C-burning (^{20}Ne) as well as small amounts of unburned matter at the surface. The central Fe-group composition depends on Y_e which is directly related to the amount of electron capture on free protons and nuclei.

as slow as a few percent of the sound speed v_s in the central regions of the white dwarf.

After an initial deflagration in the central layers, the deflagration might turn into a detonation (supersonic burning front) at larger radii and lower densities [122,169]. However, this point has initiated a strong debate. On the one hand, self-consistent, multi-dimensional calculations seem to lead to a stabilization of the deflagration burning front velocity in terms of the laminar flame velocity. This results in total in burning products of only about 0.4 $M_\odot$ of ^{56}Ni, coupled to a total explosion energy of $(5-6)\times10^{50}$ erg [73,204] and a substantial mass of unburned C and O. This seems to contradict supernova observations requiring vanishing amounts of unburned matter. The question remains how this stabilization can be broken and how a transition to active turbulent combustion, causing a detonation, can occur. One option seems to be the existance of shear instabilities caused by the angular motion of accreted matter onto the white dwarf [239,100].

Keeping these uncertainties in mind, it is possible to perform 1D spherically symmetric calculations which parametrize the lack in knowledge of (a) the binary accretion history by chosing a central ignition density $\rho_{\rm ig}$ (of the order 10^9 g/cm^3), (b) the propagation of the deflagration front by chosing a prescription for the deflagration velocity $v_{\rm def}$ (of the order of a few % of the sound velocity), and (c) the density $\rho_{\rm tr}$ where a transition from a deflagration to a detonation takes place (of the order 10^7 g/cm^3). Fig. 1 shows the resulting abundance composition of such a calculation [27,232].

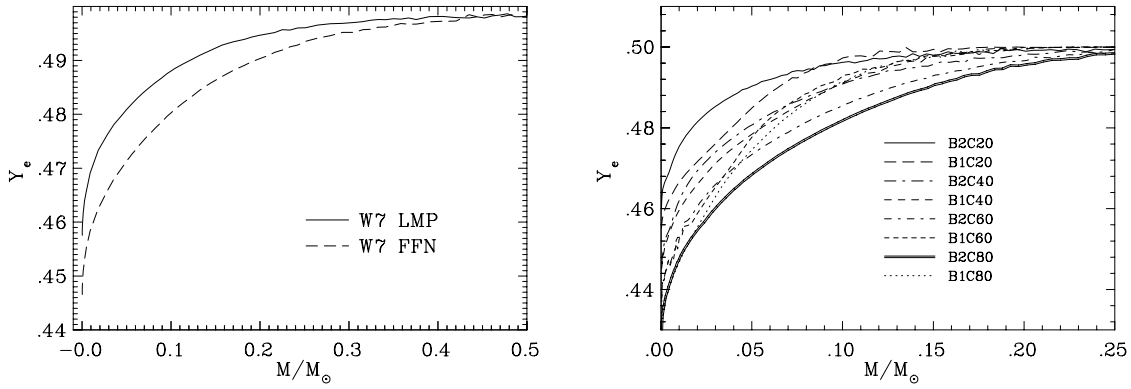

Figure 2. $Y_e =< Z/A >$ after freeze-out of nuclear reactions measures the electron captures on free protons and nuclei [27,232]. Left: A change in the set of electron capture rates from FFN to LMP reduced the amount of electron capture and leads to less neutron-rich matter in the central part. Right (calculated with LMP): Small burning front velocities lead to steep Y_e-gradients which flatten with increasing velocities (see the series of B1 vs. the B2 models). Lower central ignition densities shift the curves up (see changes from C20 through C80, i.e. central ignitions at 2-8$\times 10^9$ g cm^{-3}), but the gradient is the same for the same propagation speed.

2.2. The Role of Nuclear Physics

The outcome is not only dependent on $\rho_{\rm ig}$, $v_{\rm def}$, and $\rho_{\rm tr}$. The nuclear reaction rates entering the thermonuclear modeling can play an important role. While large central portions of the ejecta which experience maximum temperatures in excess of 5×10^9 K follow nuclear statistical equilibrium (a chemical equilibrium of all strong and electromagnetic reactions), weak interactions occur on a longer timescale and different choices affect the results strongly [70] (FFN), [133] (LMP). Electron capture affects the central electron fraction Y_e which depends on (i) the electron capture rates of nuclei directly, (ii) $v_{\rm def}$, influencing the time duration of matter at high temperatures (and with it the availability of free protons for electron captures), and (iii) the central density of the white dwarf $\rho_{\rm ig}$ (increasing the electron chemical potential i.e. the Fermi energy). The nucleosynthesis consequences are shown for the innermost about 0.2 $M_\odot$ in Fig. 2. A major effect is that contrary to initial claims [111], the change in electron capture rates permits ignition densities expected from binary stellar evolution [26,27,232]. The general nucleosynthesis outcome of SNe Ia is dominated by Fe-group products, but involves sizable fractions of Si-Ca and minor amounts of unburned or pure C-burning products (e.g. C, O, Ne, Mg). The ratio of Fe to Si-Ca is about a factor of 2-3 higher than in solar composition [82].

2.3. 3D Models

The future will lie in a consistent modeling in 3D of SNe Ia [202,73,204] rather than parametrized 1D calculations presented here. The nucleosynthesis constraints on e.g. ^{54}Fe and ^{58}Ni will have to be met by these models as well and might also lead to insight into the exact working of Ia explosions [238]. While uncertainties of the detailed 3D burning

front propagation have been parametrized in 1D models in terms of $v_{\rm def}$ and $\rho_{\rm tr}$, it is expected that in a self-consistant simulation both "parameters" will adjust themselves to unique values for the same initial models. $\rho_{\rm ig}$ is a system indicator, reflecting the accretion history in a binary system. A similar hidden system parameter is the mass of the initial white dwarf, which determines the C/O ratio within the original white dwarf before accretion sets in [57]. The accretion burning at higher temperatures during the pre-explosion evolution leads always to comparable C and O mass fractions in the outer layers.

3. Type II Supernovae

3.1. The Mechanism

The problem of core collapse supernova explosions is an old one and the attempt to understand the mechanism has been ongoing for more than 30 years. The idea that a massive star proceeds through all burning stages from H to Si-burning, finally leading to the collapse of the resulting Fe-core to nuclear densities (see Fig. 3) by the formation of a neutron star has long been discussed [14,179,9]. Since the sixties the explosion mechanism has been related to neutrino emission from the hot collapsed core [48,21,20], interrupted by a period when it was speculated that the strength of the bounce at nuclear densities could permit shock waves with sufficient energies to lead to prompt explosions [16,15]. The equation of state is essential for setting up the conditions for the later neutrino transport phase, but a pure bounce shock explosion could not be verified after previously neglected neutrino scattering processes were introduced (e.g. neutrino-electron scattering). They permitted to replace lost low energy neutrinos, leading to a continuous energy leakage and to the death of the prompt shock within 10 ms after bounce [31,166].

Since then, and with the first neutrino detection from a core collapse supernova (SN1987A, see e.g. [128,35]), the hope has been that further improvement would lead to successful explosions via energy deposition through neutrino and anti-neutrino captures on neutrons and protons ($\nu_e + n \rightarrow p + e^-$, $\bar{\nu}_e + p \rightarrow n + e^+$). Two different paths were explored. 1. Convective instabilities, but with still simplified neutrino transport, causing either (a) convective transport in the core and leading to higher neutrino luminosities [121,21,151] or (b) higher energy deposition efficiencies in convective regions [151,114,91,69]. 2. Improved neutrino transport schemes, leading to higher neutrino luminosities via the full solution of the Boltzmann transport equation for neutrino scattering and neutrino reactions [160,158].

However, recent years have shown that with the present knowledge of physical processes a supernova explosion cannot be explained in 1D spherically symmetric nor 2D rotationally symmetric radiation-hydro calculations [196,162,140,141,33,113,93,132,235] (see Fig.4). The details of collapse onset and the conditions at bounce clearly show variations with the recent change in electrons captures and beta-decayes for pf-shell and heavier nuclei already discussed in the late stages of stellar evolution and type Ia supernovae. The new aspect in comparison to the latter two cases where the new electron capture rates show a drastic decrease in comparision to earlier phenomenological treatments is that at high densities for neutron-rich conditions the Pauli-blocking of electron captures at N=40 does not apply anymore. This is due to thermal excitations and correlations [132,93].

This leaves us with two dilemmas. First of all, the fundamental one that the supernova

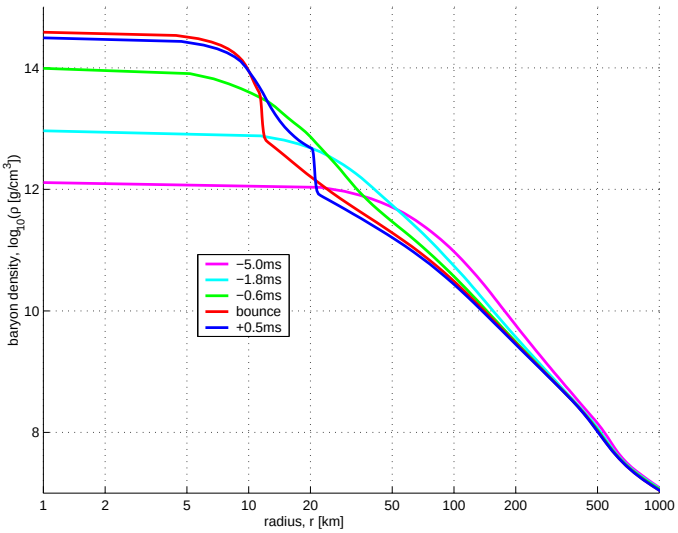

Figure 3. A sequence of density profiles of a 13 $M_\odot$ star before and after core bounce. For such a relatively low mass supernova with a small Fe-core the bounce occurs at a maximum density of less than twice nuclear matter density. At bounce one recognizes the size of the homologous core (with roughly constant density). After bounce the emergence of an outward moving density (shock) wave can be witnessed [141].

mechanism is still not understood. Second, there seems no way to predict the correct supernova nucleosynthesis yields. This is a problem for itself, but also for the strongly expanding field of galactic chemical evolution calculations, being energized by the large amount of upcoming abundance observations from low metallicity stars [5,6,216,41,103].

3.2. Nucleosynthesis Constraints

Supernova nucleosynthesis predictions have a long tradition [251,230,253,231,174,201, 45]. But all of these predictions relied on an artificially introduced explosion, either via a piston or a thermal bomb [11] introduced into the progenitor star model. While this approach makes sense and is fully correct for the outer stellar layers, provided we know the correct explosion energy to be dumped into the shock front (on the order of 10^{51} erg seen in observations), it clearly is incorrect for the innermost ejected layers which should be directly related to the physical processes causing the explosion. This affects the Fe-group composition [82], discussed in detail in [231], which was also recognized as a clear problem by [45]. The problem is also linked to the so-called neutrino wind, emitted seconds after the supernova explosion, and considered as a possible source of the r-process to produce the heaviest elements via neutron captures [224,254,193,234,245,225,235].

The dominant quantity to describe nucleosynthesis correctly in the innermost ejecta is the $Y_e = \langle Z/A \rangle$ in the layers undergoing explosive Si-burning. This Y_e is set by the weak interactions in the explosively burning layers, i.e. electron and positron captures, beta-decays, and neutrino or antineutrino captures. The dominant reactions in hot photodisintegrated matter, consisting mainly of neutrons and protons are $\nu_e + n \leftrightarrow p + e^-$

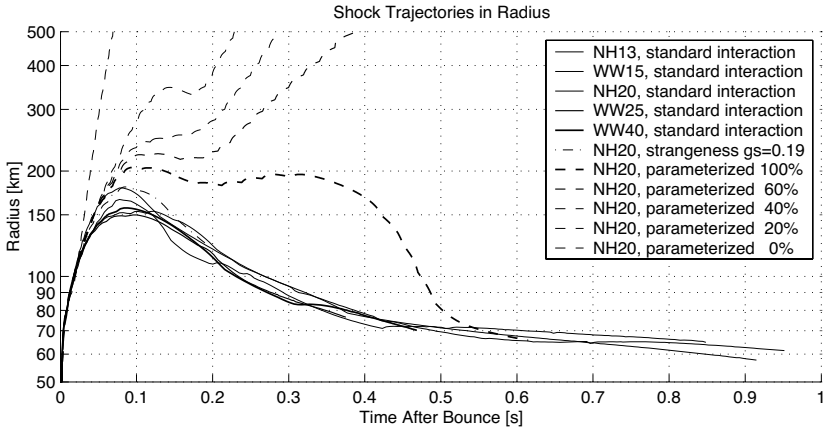

Figure 4. A sequence of collapse calculations for different progenitor masses, showing in each case the radial position of the shock front after bounce as a function of time [68]. We see that the shocks are strongest for the least massive stars. But in these 1D calculations all of them stall, recede and turn into accretion shocks, i.e. not causing successfull supernova explosions. A reduction in neutrino-nucleon elastic scattering, leading to higher luminosities, can cause explosions (performed for a $20M_\odot$ star).

and $\bar{\nu}_e + p \leftrightarrow n + e^+$. Fig. 5 shows (for calculations described below) that these reactions approach an equilibrium for Y_e on a time scale comparable to the dynamics. It also shows that the resulting Y_e in the innermost ejected layers is close to 0.5, in some areas even exceeding 0.5. This has been strongly postulated as a requirement in order not to violate abundance constraints from galactic evolution and solar abundances [231]. The question arises how one can obtain realistically this behavior, given the existing problems with self-consistent explosions.

3.3. Future Prospects

Discussed improvements which could lead to successful supernova explosions are rotation and magnetic fields [233,236], uncertainties in neutrino opacities [37] or other microphysics properties and/or a detailed high resolution 3D hydrodynamic treatment of all of the above. All of these effects can introduce additional mixing in the proto-neutron star or at the neutrino sphere and would thus have an effect on convective transport or change the neutrino luminosity via improved opacities. This leads to the two options for successful explosion as discussed above: (a) enhanced neutrino luminosities or (b) enhanced deposition efficiencies for neutrino capture in convective layers. These effects can be simulated in two ways: (a) Boosting the neutrino luminosity via a scaling (reduction) of the neutrino scattering cross section on nucleons while keeping the electron/positron and neutrino/antineutrino capture cross sections on neutrons and protons at their original values. (b) Boosting the energy deposition efficiencies by enhancing the neutrino and antineutrino captures on neutrons and protons. We cannot claim that this is a self-consistant treatment, but no external energy is required to produce a successful explosion with a consistently emerging mass cut between neutron star and ejecta. Moreover, our treat-

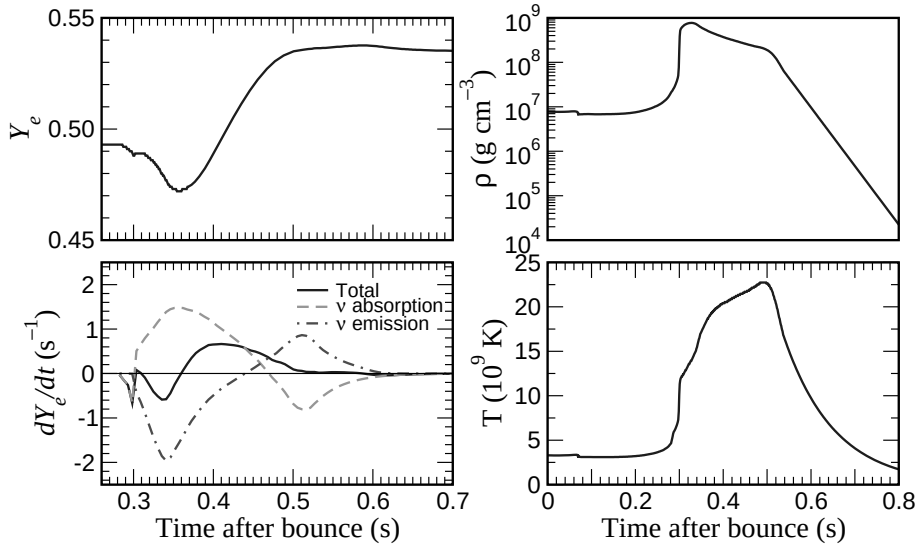

Figure 5. Hydrodynamic simulations with varied (reduced) neutrino opacities (scattering cross sections on nucleons reduced by 60%) lead to larger neutrino luminosities and make successful supernova explosions possible [68]. Here we see the time evolution after core bounce of the innermost ejected layer from a $20M_\odot$ supernova progenitor. Y_e=<Z/A> indicates the neutron-richness of ejected matter, dY_e/dt the time derivative due to the different reactions involving free protons and neutrons $\nu_e + n \leftrightarrow p + e^-$ and $\bar{\nu}_e + p \leftrightarrow n + e^+$ in the directions of neutrino (and antineutrino) absorption or emission. $\rho(t)$ and $T(t)$ the indicate density and temperature. What can be noticed is that Y_e is strongly dependent on both neutrino absorption and emission reactions and that apparently in these exploding models Y_e in the innermost zones is larger than 0.5, i.e. proton-rich.

ment guarantees that Y_e is consistently determined by all weak interactions processes. The result is that in both cases (a) and (b) explosions are obtained, as seen in Fig.4 and the neutrino interaction with matter leads to a Y_e enhanced beyond 0.5 (see Figs. 5 and 6 from [68]) which overcomes nucleosynthesis problems for the Fe-group encountered previously [230,231].

To summarize at this point. The major nuclear physics ingredients with a strong influence on core collapse supernovae are related to electron captures on nuclei, the nuclear equation of state, and neutrino-nucleon/nucleus/ nuclear matter interactions. Nucleosynthesis details are of course also related to a variety of reaction cross sections [226,102] as well as neutrino-nucleus reactions [89].

4. The r-Process

4.1. Basics

The heavy elements in nature are made by neutron capture and (at least) two types of different environments are required [34,39]. (i) A process with small neutron densities, experiencing long neutron capture timescales in comparison to β-decays ($\tau_\beta < \tau_{n,\gamma}$, slow

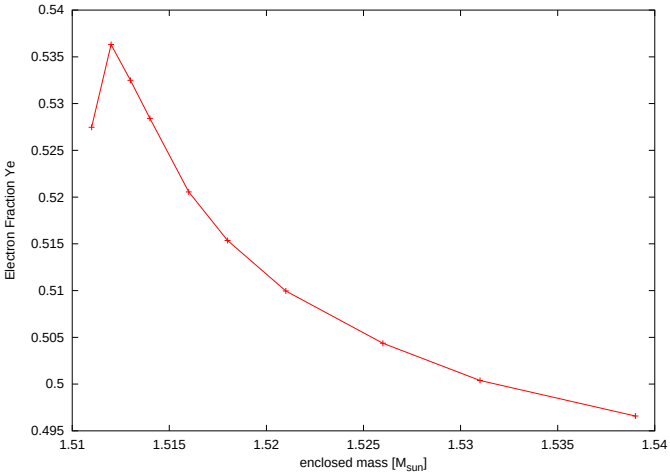

Figure 6. Y_e of the innermost ejecta due to neutrino interactions with matter via $\nu_e + n \leftrightarrow p + e^-$ and $\bar{\nu}_e + p \leftrightarrow n + e^+$. At high temperatures electrons are not degenerate, thus the reduction of Y_e due to electron captures is ineffective. For similar neutrino and antineutrino spectra the neutron-proton mass difference favors the first reaction over the second.

neutron capture or the s-process), causes abundance peaks in the flow path at nuclei with small neutron capture cross sections, i.e. stable nuclei with closed shells at magic neutron numbers [115,7] (as discussed in section 1.2 as a consequence of (α, n)-reactions in stellar He-burning). (ii) A process with high neutron densities and temperatures, experiencing rapid neutron captures and the reverse photodisintegrations with $\tau_{n,\gamma}, \tau_{\gamma,n} < \tau_\beta$, causes abundance peaks due to long β-decay half-lives where the flow path comes closest to stability (also at magic neutron numbers, but for unstable nuclei).

In the latter case an $(n,\gamma)\rightleftharpoons(\gamma,n)$ equilibrium exists if neutron captures and photodisintegrations are fast in comparison to beta-decays between isotopic chains, leading to a distribution of abundances in each isotopic chain governed by a chemical equilibrium $\mu_n + \mu_{Z,A} = \mu_{Z,A+1}$ in a Boltzmann gas. This causes abundance ratios of neighboring isotopes $Y(Z, A+1)/Y(Z, A) = f(n_n, T, S_n)$ to depend only on neutron density n_n, temperature T, and the neutron separation energy S_n (or reaction Q-value for the appropriate neutron capture) [214,129]. The maximum $Y(Z, A)$ in each isotopic chain for a given Z occurs at a universal $S_{n,max}$, being the same for all Z's. Thus, the combination of a neutron density n_n and temperature T determines the r-process path (connecting the isotopes with the maximum abundance in each isotopic chain). The $(n,\gamma)\rightleftharpoons(\gamma,n)$ equilibrium seems attained in the early phases of high neutron densities and temperatures before the freeze-out of neutron abundances and photodisintegrations (for decreasing temperatures). For small β-decay half-lives, encountered in between magic numbers, also a steady-flow of beta-decays seems applicable.

During the rapid neutron-capture process (r-process) the path passes through highly unstable nuclei with short half-lives [118], leading also to the formation of the heaviest elements in nature like Th, U, and Pu. Far from stability, neutron shell closures are

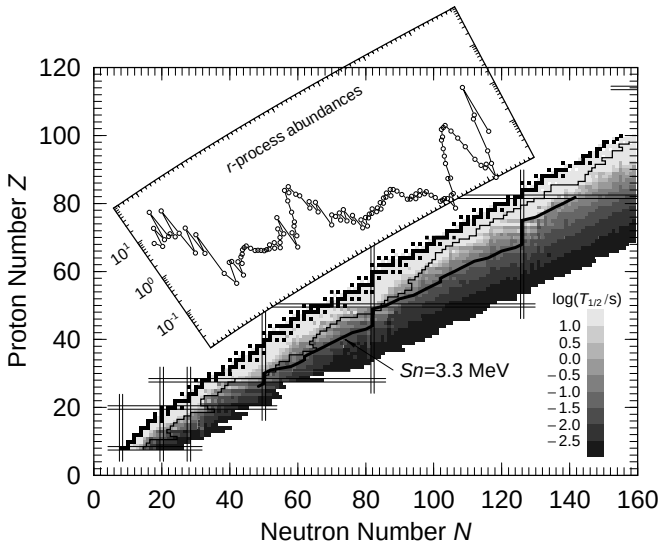

Figure 7. Some features of nuclei in the (N, Z)-chart of isotopes. Stable nuclei are indicated by black filled squares. The thin solid line represents the present limit of experimentally known nuclear masses. The magic numbers are shown as double bars. The thick solid line is the contour line of constant S_n=3.3 MeV. It relates nuclear properties to astrophysical abundances of the r-process. It can be recognized that the abundances are proportional to the β^--decay half-lives [indicated by grey shades in $\log_{10}(\tau_{1/2})$] along S_n contour lines.

encountered for smaller mass numbers A than in the valley of stability. Therefore, if r-process peaks are due to long β-decay half-lives of neutron-magic nuclei, the r-process abundance peaks are shifted in comparison to the s-process peaks (which occur for neutron shell closures at the stability line).

Site-independent classical analyses [129,50], based on neutron number density n_n, temperature T, and duration time τ, as well as entropy based calculations with the parameters entropy S, Y_e, and expansion timescale τ [101,66] have shown that the solar r-process can be fit by a continuous superposition of components with neutron separation energies (at freeze-out) in the range 4-1 MeV [50,66].

4.2. The Role of Nuclear Physics

The main aspects of an r-process are neutron captures, photodisintegrations, and β-decays.

During an r-process event exotic nuclei with neutron separation energies of 4 MeV and less are important, up to S_n=0, i.e. the neutron drip-line. These are the regions of the nuclear chart (extending to the neutron drip-line) where nuclear structure, related to masses far from stability and beta-decay half-lifes [187] have to be investigated. Such nuclei not accessible in laboratory experiments to date but hopefully in the foreseeable future (RIKEN, GSI, RIA). The knowledge of S_n (or equivalently nuclear masses) [163,1,12,186,13] determines the r-process path. In recent years new non-relativistic or relativistic mean field approaches have been addressing this question [43,56,80,171,81,209,243,18,203]. Nevertheless, microscopic-macroscopic models, like the

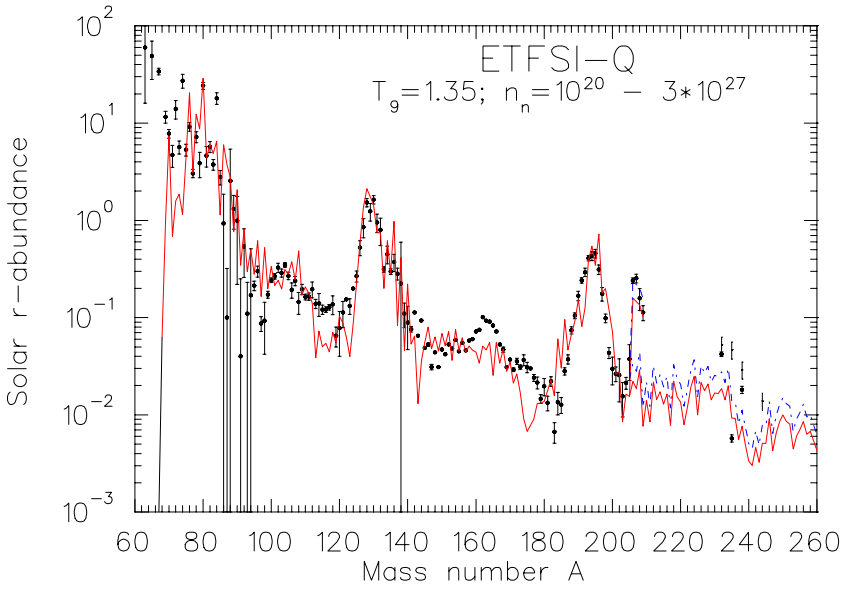

Figure 8. Fits to solar r-process abundances, obtained with two different smooth superposition of 17 equidistant $S_n(n_n, T)$ components from 1 to 4 MeV (solid and dashed lines). The ETFSI-Q mass model [186] was applied, which introduces a phenomenological quenching of shell effects. The quenching of the $N = 82$ shell gap avoids a large abundance trough below the A=130 peak. These results also show a good fit to the r-process Pb and Bi contributions after following the decay chains of unstable heavier nuclei (indicated by two sets of abundances for A>205).

FRDM [163] or the ETFSI [1,186] still seem to provide the most accurate reproduction of known masses [80].

During the r-process beta-decay half-lives determine the flow speed to heavy nuclei. After the freeze-out from $(n,\gamma)\rightleftharpoons(\gamma,n)$ equilibrium the final decay back to stability requires also the knowledge of β-delayed properties (neutron emission and fission) which can depend strongly on the beta strength-function [229,155,49,220,182,25,183]. During the freeze-out also neutron captures can still affect the final abundance pattern [222,66,61]. If the latter is the case, individual neutron capture cross sections are required [157,197,79,199,200,244].

Fission will set in during an r-process, when neutron-rich nuclei are produced at excitation energies beyond their fission barriers [228,229,49,184]. The role of β-delayed and neutron-induced fission has two aspects. For nuclei with neutron separation energies of the order 2 MeV, neutron capture will produce compound nuclei with much smaller excitation energies than those obtained in β-decay. However, the rates of neutron-induced processes (responsible also for the $(n,\gamma)\rightleftharpoons(\gamma,n)$ equilibrium) are orders of magnitude larger than beta-decay rates. Thus, it is possible that neutron-induced fission can compete with beta-delayed fission (see Fig. 9). Fission determines on the one hand the heaviest nuclei produced in an r-process [229,49,67,159,148,182–184] and on the other hand also the fission yields fed back to lighter nuclei [67,182,165].

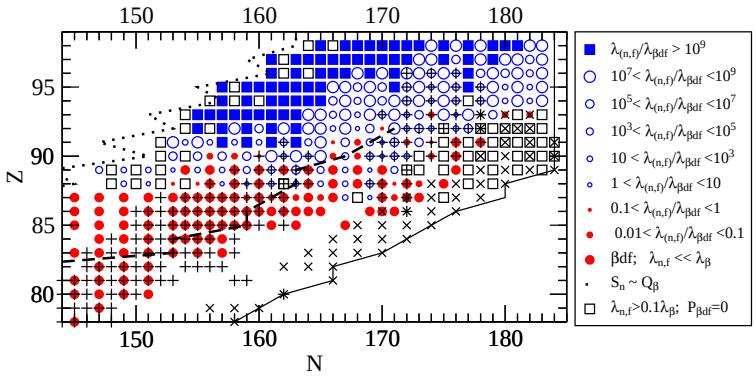

Figure 9. Ratios of neutron-induced to beta-delayed fission for nuclei of interest in r-process calculations [183]. These exploratory results were obtained with the fission barriers by Howard & Möller [104]. Different barrier heights [159,148] will lead to different total fission rates [184]. However, it was shown here that neutron-induced fission is a viable ingredient for r-process studies and should not be neglected in comparison to beta-delayed fission.

In some environments, like e.g. in supernovae, a high neutrino flux of different flavors is available. This gives rise to neutral and charged current interactions with nucleons and nuclei, i.e. elastic/inelastic scattering or electron neutrino or antineutrino capture on nuclei, e.g. $\nu_e + (Z, A) \rightarrow (Z + 1, A) + e^-$, (giving results similar to β transformations). During freeze-out the first mechanism redistributes abundances to nearby mass numbers [124,193,90,130,24,131,133] similar to spallation. Neutrino capture for high neutrino fluxes could mimic fast β^--decays, possibly accelerating an r-process to heavy elements [167,71, 152,194,156,130,131]. The effects of exotic neutrino properties are discussed in [125,153, 185].

4.3. r-Process Sites

The parameter which determines whether an r-process occurs is, the neutrons per seed ratio, see e.g. [66]. The r-process requirement of 10 to 150 neutrons per r-process seed (in the Fe-peak or somewhat beyond), permitting to produce nuclei with $A > 200$, can be translated into the parameters entropy S, Y_e and expansion timescale τ of a heated blob of material in astrophysical events, consisting of a net ratio of protons to neutrons (or total nucleons) with a given expansion history. At low entropies (without an alpha-rich freeze-out of charged-particle reactions) this is equivalent to $Y_e = <Z/A> = 0.12$-0.3. Such a high neutron excess is only possible for high densities in neutron stars under beta equilibrium ($e^- + p \leftrightarrow n + \nu$, $\mu_e + \mu_p = \mu_n$), based on the high electron Fermi energies which are comparable to the neutron-proton mass difference [154].

Deviations from this straightforward balance are only possible if one stores large amounts of mass in N=Z nuclei with small neutron capture cross sections (e.g. ^{4}He), leaving then all remaining neutrons for a few heavy seed nuclei. This phenomenon is known as an extremely α-rich freeze-out in complete Si-burning and corresponds to a weak link of reactions between the light nuclei (n, p, α) and heavier nuclei at low densities. The links

across the particle-unstable A=5 and 8 gaps are only possible via the three-body reactions $\alpha\alpha\alpha$ and $\alpha\alpha n$ to ^{12}C and ^{9}Be, whose reaction rates show a quadratic density dependence. The entropy ($\propto T^3/\rho$ in radiation dominated matter) can be used as a measure of the ratio between the remaining He mass fraction and heavy nuclei. A well known case is the big bang where under extreme entropies essentially only ^{4}He is left as the heaviest nucleus available. Somewhat lower entropies permit the production of (still small) amounts of heavy seed nuclei. Then, even moderate values of Y_e=0.4-0.5 can lead to high ratios of neutrons to heavy nuclei for entropies in excess of 200 k_B per baryon. and neutron captures can proceed to form the heaviest r-process nuclei [252,157,224,254,101,66]. These two environments represent a normal (low-entropy) and an α-rich (high-entropy) freeze-out from charged-particle reactions before the dominance of neutron-induced reactions. Towards low entropies the transition to a normal freeze-out occurs, leading to a negligible entropy dependence of the neutron to seed ratio.

If SNe II are responsible for the solar r-process abundances, given the galactic occurance frequency, they would need to eject about 10^{-5} $M_\odot$ of r-process elements per event (if all SNe II contribute equally). The scenario is based on the so-called "neutrino wind", i.e. a wind of matter from the neutron star surface (within seconds after a successful supernova explosion) caused by neutrinos streaming out from the hot neutron star [254,224,101,192, 156,180,234,225,235,259].

This high entropy neutrino wind is expected to lead to a superposition of ejecta with varying entropies. If a sufficiently high entropy range is available (for a given Y_e and expansion timescale) an r-process abundance pattern can be obtained. However, the r-process by neutrino wind ejecta of SNe II faces two difficulties. (i) Whether the required high entropies for reproducing heavy r-process nuclei can really be attained in supernova explosions has still to be verified [168,234,225,235]. Presently it seems that only (unrealistically?) large or compact neutron stars with masses in excess of 2 $M_\odot$ can provide the high entropies required. (ii) The mass region 80–110 experiences difficulties to be reproduced adequately [66,245], reflecting rather abundances determined by alpha separation energies after an alpha-rich freeze-out than neutron separation energies. It has to be seen whether the inclusion of non-standard neutrino properties [153] can cure both difficulties or lower Y_e zones can be ejected from SNe II, as recently claimed [221] from assumed prompt explosion calculations, lacking a proper neutrino transport. Present supernova models face the problem that the entropies required seem not yet attainable, unless ad hoc assumptions on reduced expansion timescales [225,259] can be verified or attained by the influence of magnetic fields [235].

An alternative site for the heavy r-process nuclei are neutron-star ejecta, like e.g. in neutron star mergers [136,60,67] or jets from supernova explosions with rotation and magnetic fields [40]. The merger of two NS leads to the ejection of neutron-rich material [112,206,208,207] of the order of $10^{-(2-3)}M_\odot$ in Newtonian and relativistic calculations [177]. The decompression of cold neutron-star matter has been studied [136,154]; however, a hydrodynamical calculation coupled with a complete r-process calculation has not been undertaken, yet. The large amount of free neutrons (up to $n_n \simeq 10^{32}$ cm^{-3}) available in such a scenario leads to the build-up of the heaviest elements and also to fission cycling within very short timescales, while the flow from the Fe-group to heavier elements "dries up". This produces to a composition void of abundances below the A$\simeq$130 peak, which

is, however, dependent on detailed fission yield predictions [183].

A discussion of the advantages and disadvantages of both possible r-process sources (SNe II vs. neutron star mergers) is given in refs. [195,207]. The two possible sites discussed above (SNe II and neutron star mergers) have different occurance frequencies and different amounts of r-process ejecta, if a successful r-process actually occurs. These properties enter into the enrichment pattern of r-process elements in galactic evolution. Inhomogeneous galactic evolution models in the very early phases of the Galaxy [110,5,6] indicate that probably neutron star mergers set in too late in galactic evolution in order to meet the observational contraints from the scatter of r-process to Fe ratios in "low metallicity stars" as a function of metallicity, i.e. the $(Fe/H)/(Fe/H)_{\odot}$ ratio.

5. Novae and X-Ray Bursts

The basic concept of a thermonuclear runaway as the driving explosion mechanism seems reasonably well understood but there are still considerable discrepancies between the predicted observables and the actual observations. The proposed mechanism involves binary systems with one (or two) degenerate objects, like white dwarfs or neutron stars and is characterized by the revival of the dormant objects via mass overflow and accretion from the binary companion. This leads to explosive events like novae and X-ray bursts. Low accretion rates lead to a pile-up of unburned hydrogen, causing the ignition of hydrogen burning via pp-chains and CNO-cycles with pycnonuclear enhancements of the reactions after a critical mass layer is attained. On white dwarfs this triggers nova events, on neutron stars it results in X-ray bursts.

5.1. Novae

Novae are identified as white dwarfs in binary systems, accreting matter from a close binary companion star in a burning stage close to main sequence H-burning with an extended envelope. [74]. The accreted material forms a thin, but high density electron degenerate layer at the surface of the white dwarf. Dredge up of white dwarf material (^{4}He, ^{12}C, ^{16}O in the case of an CO-white dwarf, ^{16}O, ^{20}Ne, and ^{24}Mg in the case of an ONeMg-white dwarf) into the envelope leads to an enrichment of the accreted material in heavier isotopes [77].

After a "critical" mass has been accreted, thermonuclear ignition takes place at the bottom of the accreted envelope. This depends critically on the mass of the white dwarf and the accretion rate which determines the pressure conditions at the bottom of the envelope. The ignition presumably occurs via the pp-chains, at degenerate electron gas conditions this causes a rapid increase in temperature at constant pressure and density. This "thermonuclear runaway" is further enhanced by the subsequent ignition of the hot CNO cycles on the high abundances of ^{12}C and ^{16}O until the degeneracy is lifted.

Typical novae are characterized by thermal runaways with densities of approximately $\rho \approx 10^3$ g/cm^3 and typical peak temperatures between $1{\cdot}10^8$ K and $4{\cdot}10^8$ K [217]. The main observables for a reliable interpretation of the explosion mechanisms are the nova light curve and the abundance distribution in the ejected material. For a reliable interpretation of such observations improved nuclear physics input in the present nova models is crucial. The actual ignition temperature for novae is well below these peak temperatures. The main energy generation in nova comes from the hot (or β-limited) CNO cycles

^{12}C(p,γ)^{13}N(p,γ)^{14}O(β,ν)^{14}N(p,α)^{15}O(β,ν)^{15}N(p,α)^{12}C and is determined by the rather long life times of the ^{14}O and ^{15}O oxygen isotopes. The actual energy generation rate is limited by the β-decay rates but is also affected by the hydrogen and CNO fuel available. In addition, the fuel balance may also change due to additional proton capture processes on short-lived radioactive nuclei in the CNO range [249]. Of particular relevance are the time scales for reaction sequences like ^{16}O(p,γ)^{17}F(p,γ)^{18}Ne(β,ν)^{18}F(p,α)^{15}O which would control fast additional fuel supply for the hot CNO cycle. Detailed sensitivity studies on explosive hydrogen burning in novae as a function of such nuclear uncertainties have been performed in a number of recent articles [119,218,46,120,109].

Observations of over-abundances in the Ne to S mass range characterize Ne-novae which are interpreted to be thermonuclear runaways on accreting O-Ne white dwarfs (which experienced also core C-burning before turning into a white dwarf) with infusion of oxygen and neon (and magnesium) into the accreting envelope [144,76]. Proton capture reactions on the initial ^{20}Ne and ^{24}Mg lead to the production of heavier isotopes up to ^{32}S. This agrees well with recent observations in nova ejecta of silicon and sulfur [219]. According to theoretical model simulations considerable production of the long-lived radioisotopes ^{22}Na and ^{26}Al is expected [217,119] in Ne novae. However, recent observations of the gamma activity in novae with the COMPTEL observatory gave no indication for ^{22}Na or ^{26}Al activity. There is an order of magnitude discrepancy between predicted and observed intensities of the ^{22}Na gamma ray [191]. Studies of the nuclear reactions crucial to the synthesis of these radioisotopes are therefore particularly important. Recently a series of self-consistent calculations for nova nucleosynthesis have been performed for different sets of nuclear reaction rates [219,62]. The results clearly indicate significant impact of nuclear reaction rates on fast nova nucleosynthesis. Many of the reaction rate uncertainties have to be reduced in order to predict more reliable O, F, Ne, Na, Mg, Al, Si, S, Cl, and Ar abundances [109]. The most critical open questions are related to the cross sections ^{13}N$(p,\gamma)^{14}$O, ^{17}F$(p,\gamma)^{18}$Ne, ^{18}F$(p,\alpha)^{15}$O, ^{22}Na$(p,\gamma)^{23}$Mg, ^{23}Mg$(p,\gamma)^{24}$Al, ^{25}Al$(p,\gamma)^{26}$Si, and ^{26g,m}Al$(\alpha,\gamma)^{27}$Si [250].

5.2. X-Ray Bursts

X-ray bursts are explained as thermonuclear runaways in the hydrogen rich envelope of an accreting neutron star [223,139]. Low accretion rates favor a sudden ignition of the material with a rapid spread over the neutron star surface [22]. During the phase between two outbursts "quiet" pp- and CNO-cycling dominates with additional reactions on the "ashes" of the previous burst(s). The thermonuclear runaway is triggered by the ignition of the break-out reactions from the hot CNO cycles and the triple-alpha reaction [249,250]. Therefore the on-set of the X-ray burst critically depends on the rates of the alpha capture reactions on ^{15}O and ^{18}Ne. The rates for these break-out reactions carry still considerable uncertainties [149,78] and are subject to intense experimental studies using a wide variety of techniques with stable and radioactive beams [29,83,53]. The ^{15}O$(\alpha,\gamma)^{19}$Ne(p,γ)^{20}Na reaction sequence represents the main link by which the initial CNO isotopes will be converted towards heavier elements. With the onset of the ^{14}O(α,p)^{17}F reaction [42,84,257] a continuous flow of ^{4}He towards ^{21}Na via the sequence ^{4}He$(2\alpha,\gamma)^{12}$C(p,γ)^{13}N(p,γ)^{14}O (α,p)^{17}F(p,γ)^{18}Ne(α,p)^{21}Na by-passes the ^{15}O(α,γ) link and ^{18}Ne(α,p)^{21}Na emerges as the main break-out reaction controlling the flow towards heavier masses.

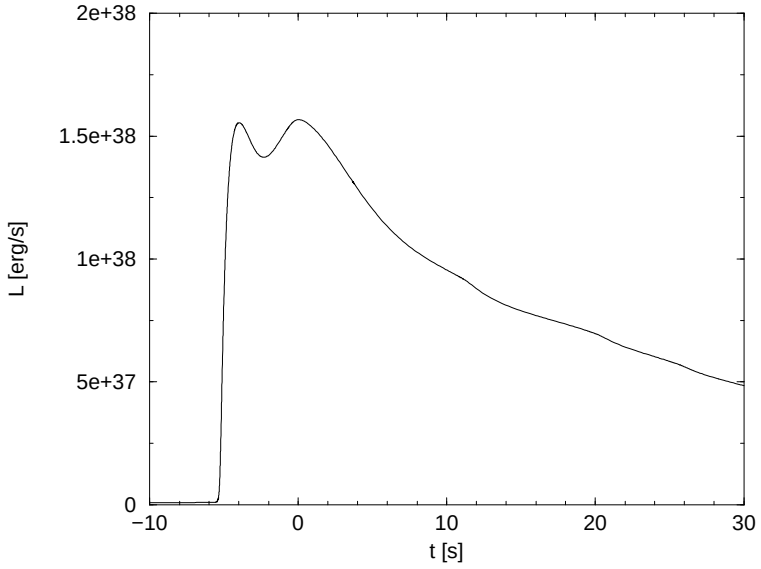

Figure 10. Luminosity profile of an X-ray burst calculation with a full nuclear network, assuming a neutron star of $1.4M_{\odot}$ and a mass accretion rate of. The double peak structure (often seen in observations) is here due to the waiting point ^{30}S [64]. Variations in neutron star size and accretion rate can change this structure, producing a regular single burst peak as well.

The thermonuclear runaway itself is driven by the αp-process and the rapid proton-process (short rp-process) which convert the initial material rapidly to ^{56}Ni causing the formation of Ni oceans at the neutron star surface. The αp-process is characterized by a sequence of (α,p) and (p,γ) reactions processing the ashes of the hot CNO cycles ^{14}O and ^{18}Ne up to ^{34}Ar and ^{38}Ca. Except for $^{14}\mathrm{O}(\alpha, p)^{17}\mathrm{F}$ and $^{18}\mathrm{Ne}(\alpha, p)^{21}\mathrm{Na}$ the reaction rates are all based on Hauser Feshbach predictions. The validity of the statistical approach in this mass range remains to be tested. This in particular since pronounced α-cluster structure in the T=1 even-even nuclei near the α threshold may lead to the occurrence of pronounced low energy resonances. Waiting points at positions where nuclear reaction flows are halted for beta-decay lifetimes, because (p, γ)- and α-induced reactions are either not competitive or overbalanced by a faster reverse reaction, have the potential to be observed in the detailed peak structure of X-ray lightcurves [64] as shown in Fig.10.

The rp-process represents a sequence of rapid proton captures up to the proton drip line and subsequent β-decays of drip line nuclei processing the material from the argon, calcium range up to ^{56}Ni and beyond. The flow is halted at ^{56}Ni during peak temperatures of around 2.0 to 3.0 billion degrees because of a $(p, \gamma) - (\gamma, p)$ chemical equilibrium due to a small reaction Q-value. In the subsequent cooling phase of the explosion photodisintegrations are suppressed and the rp-process continues beyond ^{56}Ni. The nucleosynthesis in the cooling phase of the burst alters considerably the abundance distribution in the crust of the neutron star.

To verify the present models nuclear reaction and structure studies on the neutron

deficient side of the line of stability are essential [211]. Measurements of the break-out reactions will set stringent limits on the ignition conditions for the thermonuclear runaway, measurements of alpha and proton capture on neutron deficient radioactive nuclei below ^{56}Ni will set limits on the time-scale for the actual runaway but will also affect other macroscopic observables. Recent simulations of the X-ray burst characteristics with self-consistent multi-zone models suggest indeed a significant impact of proton capture reaction rates between A=20 and A=64 on expansion velocity, temperature and luminosity of the burst [63,256]. The presently suggested reaction rates carry enormous uncertainties [211,257,107]. Recent shell model based calculations of proton capture rates in this mass range [62] did indeed indicate up to several orders of magnitude discrepancies to the global Hauser Feshbach predictions [211,199,200]. Clearly, more experimental data are necessary to remove the present uncertainties.

Nuclear structure determines the conditions for the flow to heavier nuclei in the cooling phase. In particular the experimental study of 2-proton capture reactions bridging the drip-line for even-even $N = Z$ nuclei like ^{64}Ge, ^{68}Se and ^{72}Kr are necessary to determine the final fate of the neutron star crust. The 2p-capture rates depend sensitively on the proton binding energies of the ^{65}As, ^{69}Br and ^{73}Rb nuclei, therefore reliable mass measurements are necessary for nuclei along the proton drip line in this mass range [30]. These mass measurements have to be complemented with decay studies. Of particular importance are beta-decay studies of isomeric and/or thermally populated excited states, which are not accessible for experiment with present equipment. In particular capture reactions on isomeric states may cause a significant change in reaction flow. There is a substantial need for nuclear structure information at the proton drip line, especially in the mass region along the drip line up to the A=100 range [118], to adress the multitude of open questions on the nucleosynthesis path and pattern in the rp-process towards its endpoint.

Alpha decay studies in the mass range above ^{100}Sn suggest that the neutron deficient isotopes ^{106}Te to ^{108}Te and ^{108}I predominantly decay into the α channel [181]. The isotope ^{109}I has been identified as a short-lived proton emitter [75]. This suggests that the actual endpoint of the rp-process can be associated to back-cycling of material via proton or γ induced alpha-decay in the Sn, Sb, Te range near the proton drip line. The most likely processes are ^{104}Sb$(p,\alpha)^{101}$Sn or ^{105}Te$(\gamma,\alpha)^{101}$Sn, ^{105}Sb$(p,\alpha)^{102}$Sn or ^{106}Te$(\gamma,\alpha)^{102}$Sn, and possibly also ^{106}Sb$(p,\alpha)^{103}$Sn [163,1,212].

This review would not have been possible without discussing and presenting results from joint collaborations with J.J. Cowan, W.R. Hix, P. Höflich, F. Käppeler, K.-L. Kratz, K. Langanke, M. Liebendörfer, G. Martinez-Pinedo, A. Mezzacappa, K. Nomoto, B. Pfeiffer, S. Rosswog, J.W. Truran, and M. Wiescher.

REFERENCES

1. Aboussir, Y. et al. 1995, At. Data Nucl. Data Tables 61, 127
2. Adelberger, E.G. et al. 1998, Rev. Mod. Phys. 70, 1265
3. Ahmad, Q.R. et al. 2002, Phys. Rev. Lett. 89, 011301
4. Angulo, C. et al. 1999, Nucl. Phys. A. 656, 3
5. Argast, D., Samland, M., Thielemann, F.-K., Gerhard, O. E. 2002, A & A 388, 842

6. Argast, D., Samland, M., Thielemann, F.-K., Qian, Y.-Z. 2004, A & A 416, 997
7. Arlandini, C. et al. 1999 Ap. J. 525, 886
8. Arnett, W.D. 1995, Ann. Rev. Astron. Astrophys. 33, 115
9. Arnett, W. D., Schramm, D. N. 1973, Ap. J. 184, L47
10. Arnett, W.D., Thielemann, F.-K. 1985, Ap. J. 295, 589
11. Aufderheide, M. B., Baron, E., Thielemann, F.-K. 1991, Ap. J. 370, 630
12. Audi, G. et al. 1997, Nucl. Phys. A 624, 1
13. Audi, G. et al. 2003 Nucl. Phys. A 729, 337; Wapstra, A.H., Audi, G. 2003, Nucl. Phys. A 729, 129
14. Baade, W. Zwicky, F. 1934, Proceedings of the National Academy of Science, 20, 259
15. Baron, E. et al. 1987, Phys. Rev. Lett. 59, 736
16. Baron, E., Cooperstein, J., Kahana, S. 1985, Phys. Rev. Lett. 55, 126
17. Bell, J.B. et al. 2004, Ap. J. 608, 883
18. Bender, M., Heenen, P.-H., Reinhard, P.-G. 2003, Rev. Mod. Phys. 75, 121
19. Benlliure, J., Junghans, A.R., Schmidt, K.-H. 2002, Eur. J. Phys. A 13, 93
20. Bethe, H. A. 1990, Rev. Mod. Phys. 62, 801
21. Bethe, H. A., Wilson, J. R. 1985, Ap. J. 295, 14
22. Bildsten, L., Strohmayer, T. 1999, Physics Today 52, 40
23. Bonetti, R. et al. 1999, Phys. Rev. Lett. 82, 5205
24. Borzov, I.N., Goriely, S. 2000, Phys. Rev. C 62, 5501
25. Borzov, I. N. 2003, Phys. Rev. C 67, 025802
26. Brachwitz, F. et al. 2000, Ap. J., 536, 934
27. Brachwitz, F. 2003, Ph.D. thesis, Univ. Basel
28. Branch, D., Baron, E.A., Jeffery, D.J. 2003, Lecture Notes in Physics, 598, 47
29. Bradfield-Smith, M. et al. 1999, Phys. Rev. C 59, 3402
30. Brown, B.A., Clement, R.R.C., Schatz, H., Volya, A. 2002, Phys. Rev. C 65, 04802
31. Bruenn, S. W. 1989, Ap. J. 340, 955
32. Bruenn, S.W., Haxton, W.C. 1991, Ap. J. 376, 678
33. Buras, R., Rampp, M., Janka, H.-T., Kifonidis, K. 2003, Phys. Rev. Lett. 90, 241101
34. Burbidge, E.M. et al. 1957, Rev. Mod. Phys. 29, 547
35. Burrows, A. 1990, Ann. Rev. Nucl. Part. Sci., 40, 181
36. Burrows, A., Sawyer R.F. 1999, Phys. Rev. C59, 510
37. Burrows, A. et al. 2005, Nucl. Phys. A, in press, astro-ph/0404432
38. M. Busso et al. 2001, Astrophys. J. 557, 802
39. Cameron, A.G.W. 1957, Atomic Energy of Canada, Ltd., CRL-41
40. Cameron, A.G.W. 2001, Nucl. Phys. A 688, 289
41. Cayrel, R. et al. 2004, A & A 416, 1117
42. Champagne, A.E., Wiescher, M. 1992, Ann. Rev. Nucl. Part. Sci. 42, 39
43. Chen, B. et al. 1995, Phys. Lett. B 355, 37
44. Chieffi, A., Limongi, M., Straniero, O. 1998, Ap. J. 502, 737
45. Chieffi, A. Limongi, M. 2002, Ap. J. 577, 281
46. Coc, A. et al. 2001, Nucl. Phys. A 688, 450
47. Coc, A. et al. 2004, Ap. J. 600, 544
48. Colgate, S. A., White, R. H. 1966, Ap. J. 143, 626
49. Cowan, J.J. et al. 1991, Phys. Rep. 208, 267

50. Cowan, J.J. et al. 1999, Ap. J. 521, 194
51. Cyburt, R.H., Fields, B.D., Olive, K.A. 2003, Phys. Lett. B 567, 227
52. Dappen, W., Nayfonov, A. 2000, Ap. J. Suppl. 127, 287
53. Davids, B. et al. 2003, Phys. Rev. C 67, 012801
54. Demetriou, P., Grama, C., Goriely, S. 2002, Nucl. Phys. A 707, 253
55. Dimmelmeier, H., Font, J.A., Müller, E. 2002, A&A 388, 917
56. Dobaczewski, J. 1999, Acta Phys. Pol. B 30, 1647
57. Dominguez, I., Höflich, P., Straniero, O. 2001, Ap. J. 557, 279
58. Dorfi, E.A. 1999, JCAM 109, 153
59. Eguchi, K. et al. 2003, Phys. Rev. Lett. 90, 021802
60. Eichler, D. et al. 1989, Nature 340, 126
61. Engel, J. et al. 1999, Phys. Rev. C 60, 4302
62. Fisker, J. et al. 2001, At. Data Nucl. Data Tab. 79, 241
63. Fisker J.L. et al. 2003, Nucl. Phys. A 718 , 614
64. Fisker, J.L., Thielemann, F.-K., Wiescher, M. 2004, Ap. J. 608, L61
65. Folini, D., Walder, R., Psarros, M., Desboeufs, A. 2003, in *Stellar Atmosphere Modeling*, ASP Conf. Proc. 288, 433
66. Freiburghaus, C. et al. 1999, Ap. J. 516, 381
67. Freiburghaus, C., Rosswog, S., Thielemann, F.-K. 1999, Ap. J. 525, L121
68. Fröhlich, C. et al. 2005, Ap. J. in press, astro-ph/0410208
69. Fryer, C.L., Warren, M.S. 2004, Ap. J. 601, 391
70. Fuller, G.M., Fowler, W.A., Newman, M. 1985, Ap. J. 293, 1
71. Fuller, G., Meyer, B.S. 1995 Ap. J. 453, 792; 464, 521
72. Gallino, R. et al. 1998, Ap. J. 497, 388
73. Gamezo, V.N. et al. 2002, Sci. 299, 77
74. Gehrz, R.D., Truran, J.W., Williams, R.E., Starrfield, S. 1998, PASP 110, 3
75. Gillitzer, A. et al. 1987, Z. Phys. A 326, 107
76. Gil-Pons, P. et al. 2003, A & A 407, 1021
77. Glasner, S.A., Livne, E., Truran, J.W. 1997, Ap. J. 475, 754
78. Görres, J., Wiescher, M., Thielemann, F.-K. 1995, Phys. Rev. C 51, 392
79. Goriely, S., Khan, E. 2002, Nucl. Phys. A706, 217
80. Goriely, S. et al. 2002, Phys. Rev. C66, 4326
81. Goriely, S., Samyn, M., Bender, M., Pearson, J.M. 2003, Phys. Rev. C 68, 054325
82. Grevesse, N., Sauval, A.J.1998, Space Sci. Rev. 85, 161
83. Groombridge, D. et al. 2002, Phys. Rev. C 66, 055802
84. Harss, B. et al. 2002, Phys. Rev. C 65, 035803
85. Hashimoto, M., Iwamoto, K., Nomoto, K., 1993, Ap. J. 414, L105
86. Heger, A., Langer, N., Woosley, S.E. 2000, Ap. J., 528, 368
87. Heger, A. et al. 2001, Phys. Rev. Lett. 86, 1678
88. Heger , A., Woosley , S.E., Rauscher, T. et al. 2002 New Astron. Rev. 46, 463
89. Heger, A. et al. 2005, Phys. Lett. B 606, 258
90. Hektor, A. et al. 2000, Phys. Rev. C 6105, 5803
91. Herant, M., Benz, W., Hix, W. R., Fryer, C. L., Colgate, S. A. 1994, Ap. J. 435, 339
92. Hillebrandt, W., Niemeyer, J.C. 2000, Ann. Rev. Astron. Ap. 38, 191
93. Hix, W. R. et al. 2003, Phys. Rev. Lett.91, 201102

94. Hix, W.R., Thielemann, F.-K. 1996, Ap. J. 460, 869
95. Hix, W.R., Thielemann, F.-K. 1999, J. Comp. Appl. Math. 109, 321
96. Höflich, P., Khokhlov, A. 1996, Ap. J., 457, 500
97. Höflich, P., Wheeler, J.C., Thielemann, F.-K. 1998, Ap. J. 495, 617
98. Höflich, P., Nomoto, K., Umeda, H., Wheeler, J.C. 2000, Ap. J. 528, 590
99. Höflich, P., Stein, J. 2002, Ap. J. 568, 771
100. Höflich, P., Gerardy, C., Linder, E. et al. 2003, Lecture Notes in Physics 635, 203
101. Hoffman, R.D. et al. 1997, Ap. J. 482, 951
102. Hoffman, R.D. et al. 1999, Ap. J. 521, 735
103. Honda, S. et al. 2004, Ap. J. Suppl. 152, 113
104. Howard, W.M., Möller, P. 1980, At. Data Nucl. Data Tables 25, 219
105. Hujeirat, A., Rannacher R. 2001, New Astron. Rev. 45, 425
106. Hujeirat, A. 2004, A&A 416, 423
107. Iliadis, C., Endt, P.M., Prantzos, N., Thompson, W.J. 1999, Ap. J. 524, 434
108. Iliadis, C. et al. 2001, Ap. J. Suppl. 134, 151
109. Iliadis, C. et al. 2002, Ap. J. Suppl. 142, 105
110. Ishimaru, Y. et. al. 2002, IAU Symp. 187, 117; MPA/P13, 224 (2002)
111. Iwamoto, K. et al. 1999, Ap. J. Suppl. 125, 439
112. Janka, H.T., Ruffert, M. 1996, A&A 307, L33
113. Janka, H.-T., Buras, R., Rampp, M. 2003, Nucl. Phys. A. 718, 269
114. Janka, H.-T., Müller, E. 1996, A&A, 306, 167
115. Käppeler, F. et al. 1989, Rep. Prog. Phys. 52, 945
116. Käppeler, F. et al. 1994, Ap. J. 437, 396
117. Käppeler, F. 1999, Prog. Part. Nucl. Phys. 43, 419
118. Käppeler, F., Thielemann, F.-K., Wiescher, M. 1998, Ann. Rev. Nucl. Part. Sci. 48, 175
119. José, J., Coc, A., Hernanz, M. 1999, Ap. J. 520, 347
120. José, J., Coc, A., Hernanz, M. 2001, Ap. J. 560, 897
121. Keil, W., Janka, H.-T., Müller, E. 1996, Ap. J. 473, L111
122. Khokhlov, A.M. et al. 1999, Ap. J. 524, L107
123. Kifonidis, K., Plewa, T., Janka, H.-T., Müller, E. 2004, A&A 408, 621
124. Kolbe, E. et al. 1993, Phys. Rep. 227, 37
125. Kolbe, E. et al. 1998, Eur. J. Phys. A3, 389
126. Kolbe. E. 2000, Acta. Phys. Pol. B 31, 1237
127. Kolbe, E., Langanke, K., Martinez-Pinedo, G., Vogel, P. 2003, J. Phys. G 29, 2569
128. Koshiba, M. 1992, Phys. Rep. 220, 229
129. Kratz, K.-L. et al. 1993, Ap. J. 402, 216
130. Langanke, K., Kolbe, E. 2001, ADNDT 79, 293
131. Langanke, K., Kolbe, E. 2002, At. Data Nuclear Data Tables 82, 191
132. Langanke, K. et al. 2003, Phys. Rev. Lett. 90, 241102
133. Langanke, K., Martinez-Pinedo, G. 2003, Rev. Mod. Phys. 75, 819
134. Langanke, K., Thielemann, F.-K., Wiescher, M. 2004, Lecture Notes in Physics 651, 383
135. Lattimer, J.M., Swesty, F.D. 1991, Nucl. Phys. A535, 331
136. Lattimer, J.M. et al. 1977, Ap. J. 213, 225

137.Lattimer, J.M., Prakash, M. 2001, Ap. J. 550, 426
138.Leismann, T., Aloy, M.-A., Müller, E. 2004, Ap. J. Supp. 293, 157
139.Lewin, W.H.G., van Paradijs, J.,Taam, R.E. 1993, Space Sci. Rev. 62, 233
140.Liebendörfer, M., Mezzacappa, A., Thielemann, F.-K. 2001, Phys. Rev. D 63, 104003
141.Liebendörfer, M. et al. 2001, Phys. Rev. D 63, 103004
142.Liebendörfer, M., Rosswog, S., Thielemann, F.-K. 2002, Ap. J. Supp. 141, 229
143.Liebendörfer, M. et al. 2004, Ap. J. Suppl. 150, 263
144.Livio, M., Truran, J.W. 1994, Ap. J. 425, 797
145.Livio, M. 2001 in *Supernovae and Gamma-Ray Bursts: The Biggest Explosions since the Big Bang*, eds. M. Livio, N. Panagia, K. Sahu, Cambridge Univ. Press, p.334
146.Livne, E. et al. 2004, Ap. J. 609, 277
147.Maeder, A., Zahn, J.P. 1998, A & A 334, 1000
148.Mamdouh, A. et al. 2001, Nucl. Phys. A679, 337
149.Mao, Z.Q., Fortune, H.T., Lacaze, A.G. 1996, Phys. Rev. C 53, 1197
150.Martinez-Pinedo, G., Langanke, K. 1999, Phys. Rev. Lett. 83, 4502
151.Mayle, R. Wilson, J. R. 1988, Ap. J. 334, 909
152.McLaughlin, G., Fuller, G.M. 1996, Ap. J. 464, L143
153.McLaughlin, G.C. et al. 1999, Phys. Rev. C59, 2873
154.Meyer, B.S. 1989, Ap. J. 343, 254
155.Meyer, B.S. et al. 1989, Phys. Rev. C39, 1876
156.Meyer, B.S. et al. 1998, Phys. Rev. C58, 3696
157.Meyer, B.S. et al. 1992, Ap. J. 399, 656
158.Messer, O.E.B. et al. 1998, ApJ 507, 353
159.Myers, W.D., Swiatecki, W.J. 1999, Phys. Rev. C 60, 4606
160.Mezzacappa, A. Bruenn, S. W. 1993, Ap. J. 405, 637 & 410, 740
161.Mezzacappa, A., Messer, O.E.B. 1999, J. Comp. Appl. Math. 109, 281
162.Mezzacappa, A. et al. 2001, Phys. Rev. Lett.,1935
163.Mocelj, D. et al. 2003, Nucl. Phys. A 718, 650; 2005, Nucl. Phys. A, in press
164.Möller, P. et al. 1995, At. Data Nucl. Data Tables 59, 185
165.Möller, P., Nix, J.R., Kratz, K.-L. 1997, At. Data Nucl. Data Tables 66, 131
166.Möller, P. et al. 2001, Nature 409, 785
167.Myra, E. S., Bludman, S. A. 1989, Ap. J. 340, 384
168.Nadyozhin, D.K., Panov, I.V. 1993, in: WEIN-92. ed. T.D. Vylov (World Scientific, Singapore) p. 479
169.Nagataki, S., Kohri, K 2001, Publ. Astron. Soc. Japan 53, 547
170.Niemeyer, J.C. 1999, Ap. J. 523, L57
171.Niemeyer, J.C., Bushe, W. K., Ruetsch, G.R. 1999, Ap. J. 524, 290
172.Niksic, T. et al. 2002, Phys. Rev. C66, 4306
173.Nomoto, K., Hashimoto, M. 1988, Phys. Rep. 163,
174.Nomoto, K., Thielemann, F.-K., Yokoi, K. 1984, Ap. J. 286, 644
175.Nomoto, K. et al. 1997, Nucl. Phys. A 616, 79
176.Nomoto, K. et al. 2000, in *Type Ia Supernovae: Theory and Cosmology*, Cambridge Univ. Press, eds. J. Niemeyer & J.W. Truran, p.63 (astro-ph/9907386)
177.Nugent, P. et al. 1997, Ap. J. 485, 812
178.Oechslin, R., Rosswog, S., Thielemann, F.-K. 2002, Phys. Rev. D 65, 3005

179.Oechslin, R., Uryu, K., Poghosyan, G., Thielemann, F.-K. 2004 Mon. Not. Roy. Astron. Soc. 349, 1469
180.Oppenheimer, J. R., Snyder, H. 1939, Phys. Rev. 56, 455
181.Otsuki, K. et al. 2000 Ap. J. 533, 424
182.Page, R.D. et al. 1994, Phys. Rev. C 49, 3312
183.Panov, I.V. et al. 2001, Nucl. Phys. A 688, 587
184.Panov, I.V., Thielemann, F.-K. 2003, Nucl. Phys. A 718, 647
185.Panov, I. V. et al. 2005, Nucl. Phys. A 747, 633
186.Pastor, S., Raffelt, G. 2002, Phys. Rev. Lett. 89, 191101
187.Pearson, J. M., Nayak, R. C., Goriely, S. 1996, Phys. Lett. B387, 455
188.Pfeiffer, B., Kratz, K.-L., Thielemann, F.-K., Walters, W. B. 2001, Nucl. Phys. A 693, 282
189.Pons, J.A. et al. 1999, Ap. J. 513, 780
190.Pons, J.A. et al. 2001, Phys. Rev. Lett. 86, 5223
191.Prakash, M. et al. 1997, Phys. Rep. 280, 1
192.Prantzos, N., Diehl, R. 1996, Phys. Rep. 267, 1
193.Qian, Y.-Z., Woosley, S.E. 1996, Ap. J. 471, 331
194.Qian, Y. Z., Haxton, W. C., Langanke, K., Vogel, P. 1997, Phys. Rev. C 55, 1532
195.Qian, Y.-Z. et al. 1998, Ap. J. 494, 285
196.Qian, X.-Z. 2000, Ap. J. 534, L67
197.Rampp, M., Janka, H.-T. 2000, Ap. J. 539, L33
198.Rauscher, T., Thielemann, F.-K., Kratz, K.-L. 1997, Phys. Rev. C 57, 2031
199.Rauscher, T., Thielemann, F.-K. 2000, At. Data Nucl. Data Tables, 75, 1
200.Rauscher, T. et al. 2000, Nucl. Phys. A675, 695
201.Rauscher, T., Thielemann, F.-K. 2001, At. Data Nucl. Data Tables, 79, 47
202.Rauscher, T., Heger, A., Hoffman, R. D., Woosley, S. E. 2002, Ap. J. 576, 323
203.Reinecke, M., Hillebrandt, W., Niemeyer, J. C. 2002, A&A 391, 1167
204.Reinhard, P.-G., Bender, M. 2004, Lecture Notes in Physics 641, 249
205.Röpke, F.K., Niemeyer, J.C., Hillebrandt, W. 2003, Ap. J. 588, 952
206.Rogers, F.J., Iglesias, C.A. 1998, Space Sci. Rev. 85, 61
207.Rosswog, S.K. et al. 1999, A&A 341, 499
208.Rosswog, S., Davies, M.B. 2002, Mon. Not. R Astron. Soc. 334, 481
209.Ruffert, M., Janka, H.T. 2001, A & A 380, 544
210.Samyn, M., Goriely, S., Pearson, J.M. 2003, Nucl. Phys. A 725, 69
211.Samyn, M., Goriely, S. 2004, AIP Conf. Proc. 704, 401
212.Schatz, H. et al. 1998, Phys. Rep. 294, 168
213.Schatz, H. et al. 2001, Phys. Rev. Lett. 86, 3471
214.Seaton, M.J., Badnell, N.R. 2004, Mon. Not. Roy. Astron. Soc. 354, 457
215.Seeger, P.A. et al. 1965 Ap. J. Suppl. 97, 121
216.Shen, H. et al. 1998, Prog. Theor. Phys. 100, 1013
217.Sneden, C. et al. 2003, Ap. J. 591, 936
218.Starrfield, S. et al. 1998, Mon. Not. Roy. Astron. Soc. 296, 502
219.Starrfield, S. et al. 2000, Ap. J. Suppl. 127, 485
220.Starrfield, S. et al. 2001, Nucl. Phys. A 688, 110c
221.Staudt, A., Klapdor-Kleingrothaus, H.-V. 1992, Nucl. Phys. A 549, 254

222.Sumiyoshi, K. et al. 2001, Ap. J. 562, 880
223.Surman, R. et al. 1997, Phys. Rev. Lett. 79, 1809
224.Taam, R., Woosley, S.E., Weaver, T., Lamb, D. 1993 Ap. J. 413, 324
225.Takahashi, K., Witti, J., Janka, H.-T. 1994, A&A, 286, 857
226.Terasawa, M. et al. 2002, Ap. J. 578, L137
227.The, L.-S., Clayton, D.D., Jin, L., Meyer, B.S. 1998, Ap. J. 504, 500
228.Thielemann, F.-K., Arnett, W.D. 1985, Ap. J. 295, 604
229.Thielemann, F.-K., Metzinger, J., Klapdor, H.V. 1983,: Z. Phys. A 309, 301
230.Thielemann, F.-K. et al. 1989, in: *Fifty Years with Nuclear Fission*, ed. J.W. Behrens, A.D. Carlson (American Nuclear Society,1989) p. 592
231.Thielemann, F.-K., Hashimoto, M., Nomoto, K. 1990, Ap. J. 349, 222
232.Thielemann, F.-K., Nomoto, K., Hashimoto, M. 1996, Ap. J. 460, 408
233.Thielemann, F.-K. et al. 2004, New Astronomy 48, 605
234.Thompson, C. 2000, Ap. J. 534, 915
235.Thompson, T. A., Burrows, A., Meyer, B. S. 2001, Ap. J. 562, 887
236.Thompson, T. A., Burrows, A., Pinto, P. A. 2003, Ap. J. 592, 434
237.Thompson, T. A., Quataert, E., Burrows, A. 2005, astro-ph/0403224
238.Timmes, F.X., Woosley, S.E. 1992, Ap. J. 396, 649
239.Travaglio, C., Hillebrandt, W., Reinecke, M., Thielemann, F.-K. 2004, A & A 425, 1029
240.Uenishi, T., Nomoto, K., Hachisu, I. 2003, ApJ 595, 1094
241.Umeda, H., Nomoto, K., Yamaoka, H., Wanajo, S. 1999, Ap. J. 513, 861
242.van Eck, S., Goriely, S., Jorissen, A. et al. 2001, Nature 412, 793
243.van Eck, S., Goriely, S., Jorissen, A. et al. 2003, Astron. Astrophys. 404, 291
244.Vretenar, D., Niksic, T., Ring, P. 2003, Phys. Rev. C 68, 024310
245.Vretenar, D., Niksic, T., Paar, N., Ring, P. 2004, Nucl. Phys. A 731, 281
246.Wanajo, S., Kajino, T., Mathews, G. J., Otsuki, K. 2001, Ap. J. 554, 578
247.Wasserburg, G., Busso, M., Gallino, R. 1996, Ap. J. 466, L109
248.Weber, F. 1999, Pulsars as Astrophysical Laboratories of Nuclear and Particle Physics, IOP Publishing, Bristol
249.Wheeler, J.C., Höflich, P., Harkness, R.P., Spyromilio, J. 1998, Ap. J. 496, 908
250.Wiescher, M., Görres, J., Schatz, H. 1999, J. Phys. G: Nucl. Part. Phys. 25, R133
251.Wiescher, M. 2005, Nucl. Phys. A, this volume
252.Woosley, S. E. Weaver, T. A. 1986, Ann. Rev. Astron. Astrophys. 24, 205
253.Woosley, S.E., Hoffman, R.D. 1992, Ap. J. 395, 202
254.Woosley, S.E., Weaver, T.A. 1995, Ap. J. Suppl. 101, 181
255.Woosley, S.E. et al. 1994, Ap. J. 433, 229
256.Woosley, S.E., Weaver, T.A. 1994, in *Les Houches, Session LIV, Supernovae*, eds. S.R. Bludman, R. Mochkovitch, J. Zinn-Justin, Elsevier, p. 63
257.Woosley, S.E. et al. 2004, Ap. J. Suppl. 151, 75
258.van Wormer, L. et al. 1994, Ap. J. 432, 326
259.Wunsch, S., Woosley, S.E. 2004, Ap. J. 616, 1102
260.Yoshida, T., Terasawa, T., Kajino, T., Sumiyoshi, K. 2004, Ap. J. 600, 204